A NEW DESIGN METHOD FOR GENERATING SURROGATE KINEMATIC TRUSS ORTHOSES TO SUPPORT PATHOLOGICAL GAIT PATTERNS IN HUMAN MODEL SIMULATIONS

Steck, Patrick;
Scherb, David;
Mayer, Johannes;
Jäger, Michael;
Miehling, Jörg;
Völkl, Harald;
Wartzack, Sandro

Friedrich-Alexander-Universität Erlangen-Nürnberg

ABSTRACT

With increasing life expectancy, the risk of diseases of the central nervous system, such as cancer, strokes, etc., also increases. Strokes often result in injury to the sciatic nerve, which is responsible for controlling the calf muscles (plantar and dorsal flexors). A so-called ankle joint orthosis (AFO) helps to support the pathological gait and to avoid foot drop during gait. Passive orthoses are of particular importance for research, as they do not require additional incoming energy from outside to the orthotic system. However, current passive orthoses are often not personalized. On the one hand, because they usually have only a temporary muscle-building function and, on the other hand, because the individual design process is computationally time consuming and thus expensive. This paper presents a possibility to pre-dimension and pre-design passive orthoses fast and cost-efficiently by reducing the complexity of the model based on volume-optimized truss elements. Therefor a traditional high calculation intensive design procedure is compared with the complexity reduced model to show its effectiviness and the similarity of the results.

Keywords: Orthoses, User centred design, Lightweight design, Truss optimization, Design methods

Contact:
Steck, Patrick
Friedrich-Alexander-Universität Erlangen-Nürnberg
Germany
steck@mfk.fau.de

Cite this article: Steck, P., Scherb, D., Mayer, J., Jäger, M., Miehling, J., Völkl, H., Wartzack, S. (2023) 'A New Design Method for Generating Surrogate Kinematic Truss Orthoses to Support Pathological Gait Patterns in Human Model Simulations', in *Proceedings of the International Conference on Engineering Design (ICED23),* Bordeaux, France, 24-28 July 2023. DOI:10.1017/pds.2023.33

1 INTRODUCTION

Increased life expectancy has been one of the main factors leading to increased demand for prosthetics and orthotics in recent years (Reportlinker, 2022). For example, from 2021 to 2022, the global prosthetics and orthotics market grew by $0.33 billion. By 2030, it is expected to increase by a further US$1.68 billion. These figures are a good illustration of why optimization in orthotic design is more important than ever. However, current orthotic design methods are largely concerned with mass production because, unlike prostheses, orthoses only provide a temporary remedy for damaged body parts. Nevertheless, recent studies showed that personalized and user-tailored products are beneficial for successful and rapid treatment (Leite *et al.*, 2019). For example, optical measurement methods such as 3D scanning are increasingly being used to generate digital images of affected regions (Kumar Banga *et al.*, 2021; Štefanovič *et al.*, 2021; Tavares *et al.*, 2023). These can serve as input data for reconstructing limbs or, in the case of orthoses, matching the freeform of the structure to the body part being supported. Furthermore, the location of joint axes can be measured directly from the 3D model (Spaeth, 2006). The personalization of products leads to unique products that require an individual design process. In addition, conventional dimensioning methods can only approximate the complex freeform geometries of optimized structural responses to a limited extent. The reduction to a continuum mechanically describable structure leads to large errors. Here, numerical methods such as Finite Element Analysis (FEA) and Multi Body Simulation (MBS) are used as design tools. With these, it is possible to identify the occurring loads and to perform strength analyses. First, the designed structure is discretized into simpler elements (sheet, membrane, shell, plate, etc.) and then, the resulting displacements, forces and stresses are calculated by solving the displacement differential equations (static) or eigenvalue problems (transient) (see Figure 1).

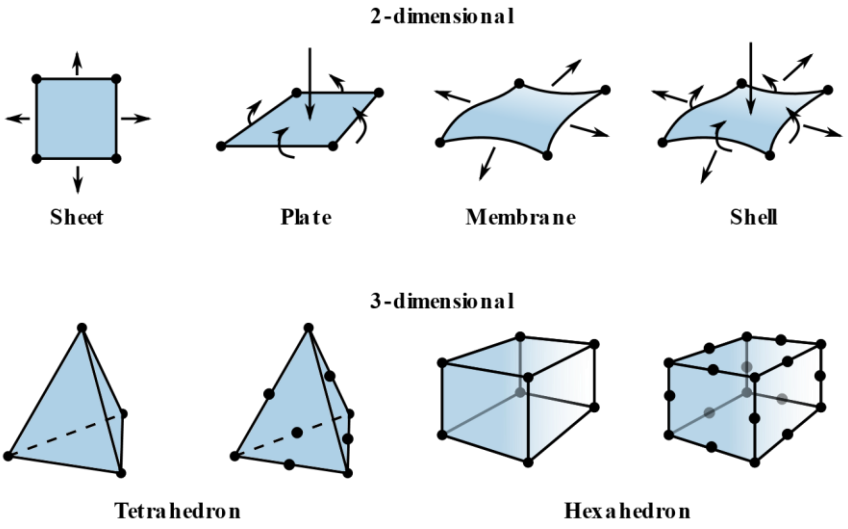

Figure 1. Overview of different element types with different number of nodes in finite element analysis.

N. P. Reddy *et al.* (1985) showed early how this form of Computer-Aided Design can be used for a passive ankle-foot orthosis (AFO). Unlike active AFO, passive ones do not require any additional energy input to the orthotic system. In the meantime, much research has been conducted in this area and sequential processes have been formulated and optimized (Chu *et al.*, 1995; Pallari *et al.*, 2010; Syngellakis and Arnold, 2012; Dickinson *et al.*, 2017; Dhokia *et al.*, 2017). A 3D-printed AFO optimized for a child with an energy-storing mechanism was designed by Banga *et al.* (2020). The authors showed that the conservative approach with shell elements is computationally very intensive. Shahar *et al.* (2019) showed the high potential of anisotropic materials for energy storage tasks for orthoses. Ali *et al.* (2021) described a similar approach to design AFO based on 3D printed CFRP structures. The use of anisotropic nonlinear materials further increases the computational time to solve the displacement ordinary differential equation (ODE), since the nonlinear effects must also be approximated. In general, the computation times scale over the third power with increasing number of element degrees of freedom (Hell, 2018). If additionally multiple targets, such as energy storage

https://doi.org/10.1017/pds.2023.33 Published online by Cambridge University Press

functions, switching processes or even coupling with musculoskeletal human models (MHM) are considered in the FEA calculation, the computation time increases exponentially. This results in a great need for optimization in the design pre-process, which leads to the research gap for a performant design and computation process in the field of personalized medical devices (Totah *et al.*, 2017; Scherb *et al.*, 2022).
The research questions are therefore:

- How can the CAD process of patient-centred orthoses be made faster and more intuitive in the future?
- And, how efficient is the presented complexity-reduced method compared to classical full models with higher-order element types?

2 METHODS

In this chapter, the overall procedure is first briefly described on the Figure 2 below. The subchapters go into detail on the used methods.

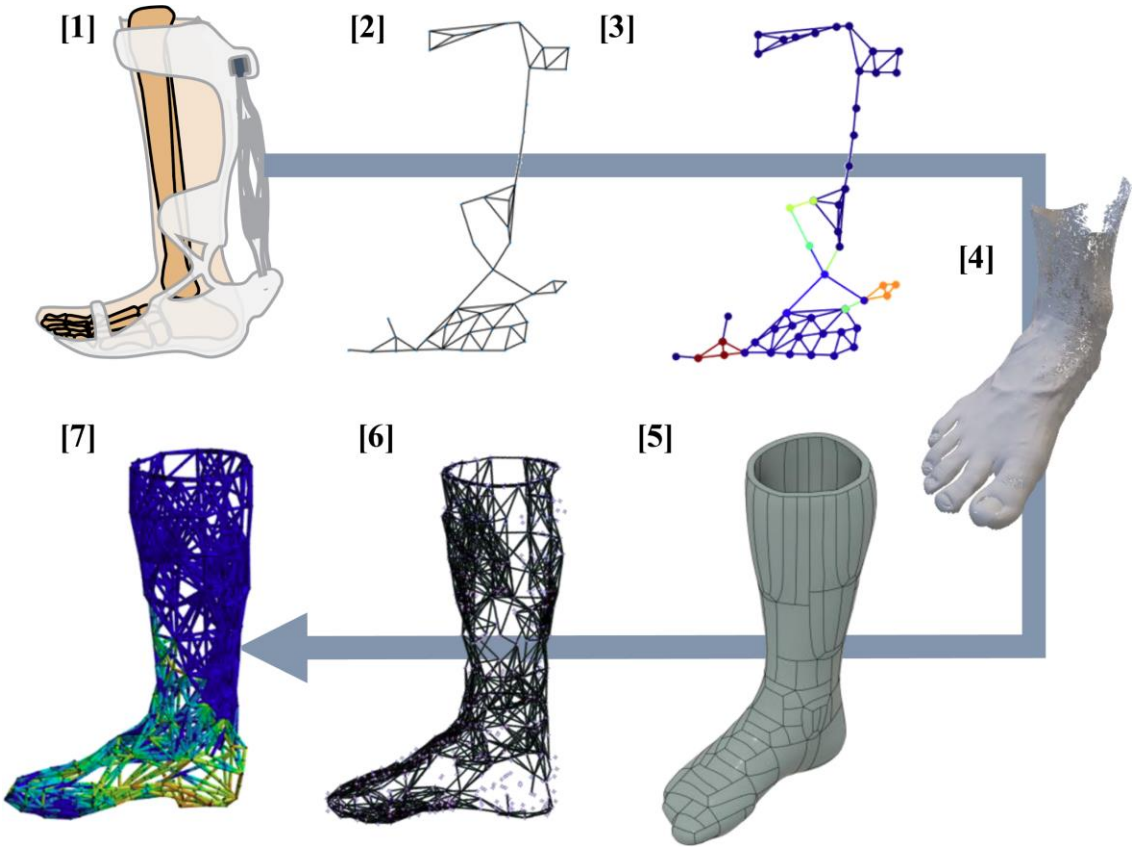

Figure 2. Procedure of the computer-aided 2D/3D truss design method for passive orthoses.

In the first step, with the help of user-centred and lightweight design specific methods, the classical design methodology according to Pahl/Beitz is applied to plan and design an AFO **[1]** (Pahl *et al.*, 2007; Miehling, 2019). The contents of the applied conceptual design methods such as requirements list, black box, structural tree as well as the exact selection of the active principles were previously published by the authors (Steck *et al.*, 2022). Subsequently, the pre-sketched orthosis is manually transformed into a 2D truss **[2]** and pre-dimensioned in a two-dimensional truss FEA (Andreas Dutzler, 2022) based on the Python package TrussPy, i.e. beam elements are distributed in the design space and the general displacement or stiffness is analysed **[3]**. For further processing, a foot is scanned at the self-test using a fringe light projection meter **[4]**. Then, in FUSION360, the orthotic concept is adapted three-dimensionally to the scanned foot **[5]**. In this step, the mechanical energy storage (if available) is also prepared. Next, the orthotic blank is thickened and transformed into a Boundary Representation object via a feature-based reconstruction (Mayer *et al.*, 2022). This serves as an input parameter for a design space, which is volume optimized in the next step (Fairclough *et al.*, 2021). The applied loads and constraint locations (Taha *et al.*, 2016; Wong *et al.*, 2016; Mitternacht and Lampe, 2006) of the orthosis

https://doi.org/10.1017/pds.2023.33 Published online by Cambridge University Press

must also be defined in this process. The optimization leads to a truss structure with minimum number of beams that just satisfies the stiffness constraint **[6]** (Jäger and Wartzack, 2023). Finally, the converged solution is validated in ANSYS with respect to its deformation or stiffness properties **[7]**.

2.1 Pre-dimensioning using two-dimensional analysis methods

As explained in chapter 1, the use of common element types (tetrahedron, hexahedron, polyhedron, see Figure 1) leads to very high computation times for this application when the number of nodes increases. Since in stiffness optimization tasks, the inversion of the global element stiffness matrix has to be recalculated in each iteration, the reduction of the number of nodes is of further importance. One of the most commonly used methods to reduce computation time in FEA is to reduce the complexity of the computational model using simpler element types such as beam or rod elements. Components or assemblies discretized with these elements are called trusses. As the results of rod elements are often non-representative about the displacement behaviour of a truss, beam elements are mostly used as best practices. Basically, a distinction is made between Bernoulli and Timoshenko beam theories (Öchsner, 2021). The first are used for long, slender beams and the second for short, thick beams. In this paper, simple 2D beams are first used for quick pre-dimensioning and Timoshenko beams are used in the further 3D design process.
First, a rough picture of a two-dimensional orthosis is sketched from a list of requirements for the various boundary conditions (see Figure 3).

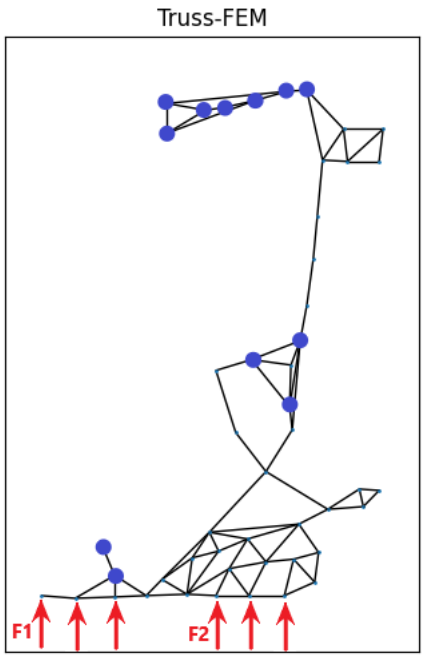

Figure 3. Load and constraint definition in 2D truss problem. F_1= 200N; F_2=400N and blue as $[u_x,u_y,u_z] = 0$

The constraints and loads are taken into account directly in the design/distribution of the beams from previously recorded gait analyses (Scherb *et al.*, 2022) for each of the four gait load cases (Heel Strike, Foot Flat, Heel Off, Toe Off) (Shorter *et al.*, 2012). A load of 400 N is applied to the heel nodes and 200 N is applied to the sole of the foot. For a body weight of 60 kg, a weight force of approximately 590 N acts at the body's centre of gravity. This force is presumed to be evenly distributed over the contact surface of one foot during gait. The heel sees about two-thirds of these surface loads (Wang *et al.*, 2018). Since point loading of a node is unlikely, the choice of loading should be considered conservatively. The orthotic truss is thus dimensioned with a safety factor S_F>1. The actual distribution is then done manually according to general design guidelines of beam trusses, i.e., arrange beams at 30-degree angles, no over-determine system, statistically distribute intermediate beams, etc. (Öchsner, 2021). Subsequently, a FEA of the 2D truss is performed. Here, the loads and restraints are distributed to the nodes according to the previously determined limit values. After that, a simple truss FE simulation was written in Python, which can solve simple 2D truss problems. The solver is basically based on the implicit solution principle $K^{-1}f = u$, i.e., after setting up the inverse global element stiffness matrix $\mathbf{K}^{-1}$

https://doi.org/10.1017/pds.2023.33 Published online by Cambridge University Press

this is reduced by zero-entries for faster calculation and subsequently offset with the given force vector **f** in a matrix multiplication. This leads to the displacement vector **u** and is the fastest way to calculate nodal displacements in the FEA. Afterwards, the displacement solution is interpreted and used as input for the three-dimensional design of the orthosis, together with the patient's foot scans.

2.2 Determination of the individual installation space by 3D scanning

In order to be able to design orthoses adapted to the patient, the patient's foot geometry data must first be recorded and integrated into the design process (see Figure 4).

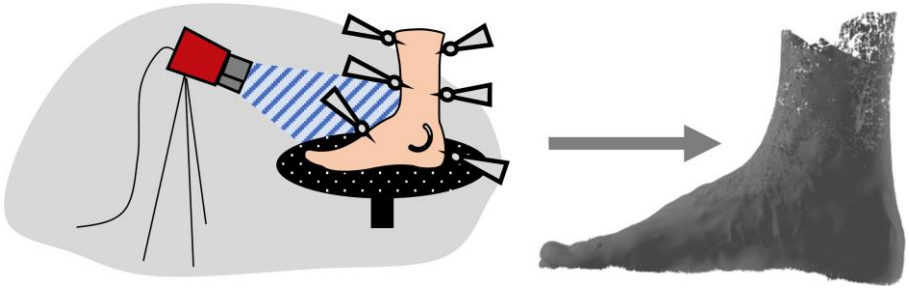

Figure 4. Schematic procedure for scanning patient feet.

A measuring device for clamping the foot and lower leg was constructed for this purpose. The difficulty here is to select as many fixed points as possible so that the foot cannot move during the measurement, but to select as few fixed points as necessary so as not to influence the measurement too much. The measurement is then performed using the strip light projection method. The gapped design space is then smoothed using Fusion 360, the gaps are closed, an offset is applied to the design space and it is re-exported as a tessellated format (.stl). In the next step, the design space is converted into a model with continuous splines (Boundary Representation Model (B-Rep)).

2.3 Design space generation with subsequent truss optimization

Next, the faceted object is changed to an B-Rep model. Here the surface representation of the model is transferred from polygonal to parametric using the approach from Mayer *et al.* (2022). The triangulated surface model is first converted to a quadrangulated surface by voxel-based remeshing in the graphics program Blender3D. The surface is approximated by voxels of manually defined size and evaluated to a polygon mesh. Subsequently, the model is imported into the CAD software Autodesk Fusion 360. The quadrangulated surfaces are automatically converted to T-spline surfaces and subsequently to the parametric surface format (see Figure 5).

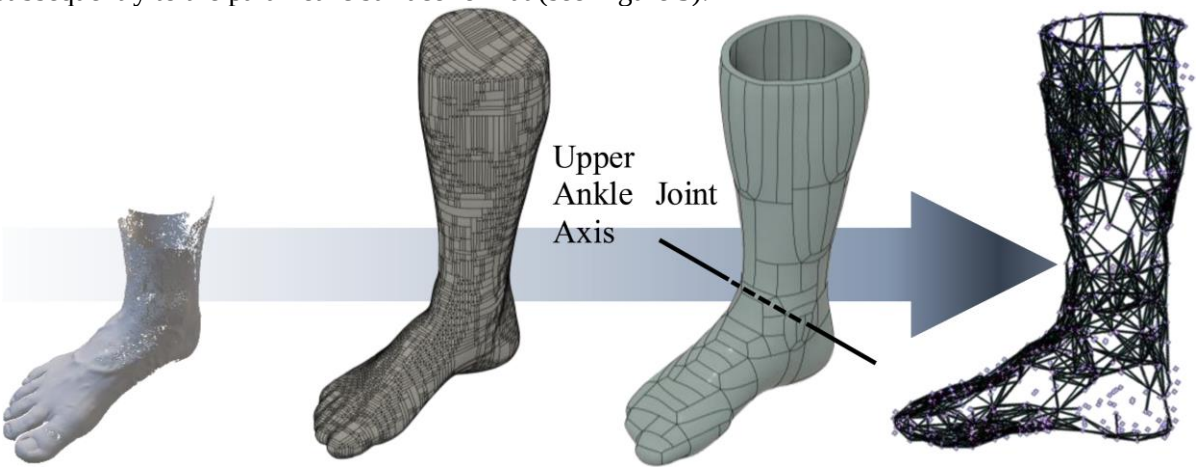

Figure 5. Workflow for the preparation of a B-Rep beam truss construction space of ankle joint orthoses.

After a 3D model has been generated, an axis is located to define the ankle moment around the upper ankle joint. This is based on the measured data and was compared to manually identified values with a Vernier calliper. Then the model can be transformed into a 3D beam truss using an approach extended

https://doi.org/10.1017/pds.2023.33 Published online by Cambridge University Press

to 3D according to Fairclough *et al.* (2021). Basically, the optimization follows the procedure in Figure 6.

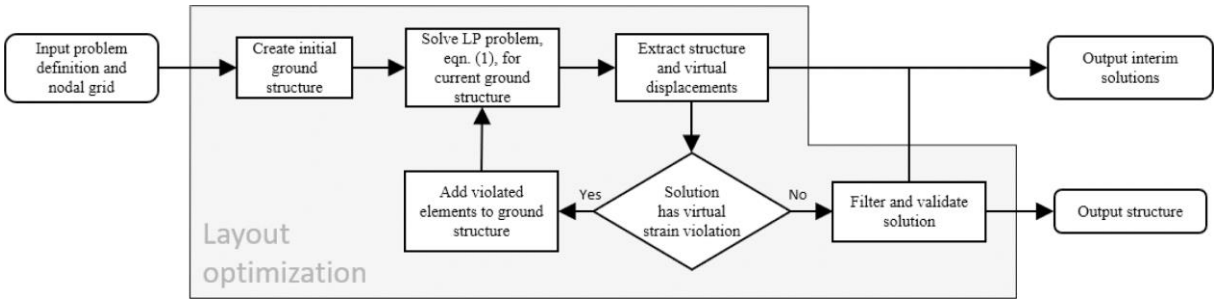

Figure 6. Layout optimization procedure for Beam-Truss-Optimization

Where the optimization problem is defined as follows:

$$\min_{\boldsymbol{a},\boldsymbol{q}^{(k)}} V = l^T a \tag{1a}$$

$$\text{subject to: } \boldsymbol{B}\boldsymbol{q}^{(k)} = \boldsymbol{f}^{(k)} \tag{1b}$$

$$-\sigma^{-}\boldsymbol{a} \leq \boldsymbol{q}^{(k)} \leq \sigma^{+}\boldsymbol{a} \tag{1c}$$

$$\boldsymbol{a} \geq 0 \tag{1d}$$

V is the volume fraction, which is the number of beams in a truss optimization. The vector $\boldsymbol{l} = [l_1, l_2, \dots, l_m]^T$ describes the length of the individual beams. The vector **a** represents the beam cross sections, which are design variables representing the density of the beams. The matrix **B** contains the directional cosines and **q**(k) the element forces for each load case k. The input vector $\boldsymbol{f}^{(k)} = [f_1^{k,x}, f_1^{k,y}, f_1^{k,z}, f_2^{k,x}, \dots, f_n^{k,(x,y,z)}]^T$ is the vector of external loads and σ^{-}/σ^{+} the admitted stresses. Since solving the optimization problem produces design variables with values close to zero but not exactly zero, filter functions must be implemented that provide the solution framework with members of constant cross-section. However, as these filter functions are not necessary for the understanding how the optimization works, they will not be discussed further here. The complete implementation follows exactly Fairclough et al. (2021) and can be found there. Finally, a solution with a minimum number of beams is obtained, which just withstands the loads. In the next step, the convergent solution is prepared for analysis in ANSYS and simulated there with respect to the occurring loads.

2.4 Validation of the deformation and stiffness behavior

In the last step, the reconstructed structure is loaded into SpaceClaim and a circular cross-section is assigned to each beam (see Figure 7).

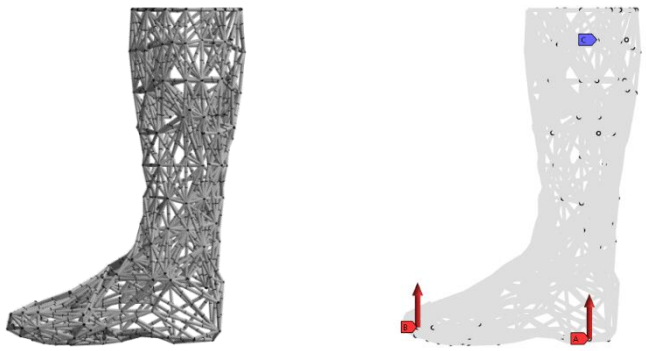

a) b)

Figure 7. 3D truss orthosis: a) Truss design suggestion after optimization process b) Load distribution and constraints on 3D truss model.

https://doi.org/10.1017/pds.2023.33 Published online by Cambridge University Press

The resulting structure is then loaded into ANSYS and the loads are applied to the defined nodes as described in the previous step. The load distributions are defined in Figure 7. The load distributions are defined and refers to the stress distribution of the 2D result by manually increasing the number of beams in the areas of high stress around the ankle joint. Then, the deformations and resulting internal element forces are analysed. Finally, the computational speed of truss optimization and ANSYS topology optimization and 3D shell elements and 3D beam elements are compared and the results are contrasted.

3 RESULTS

The methods for designing personalized truss models explained in the previous chapter are now applied to a personalized AFO. The results are presented below in Figure 8. Since stresses are vectoral quantities, values would not be representative. For this reason, the maximum stress occurring was normalized to 1. Thus, blue is a stress of 0 and red is a stress of 1.

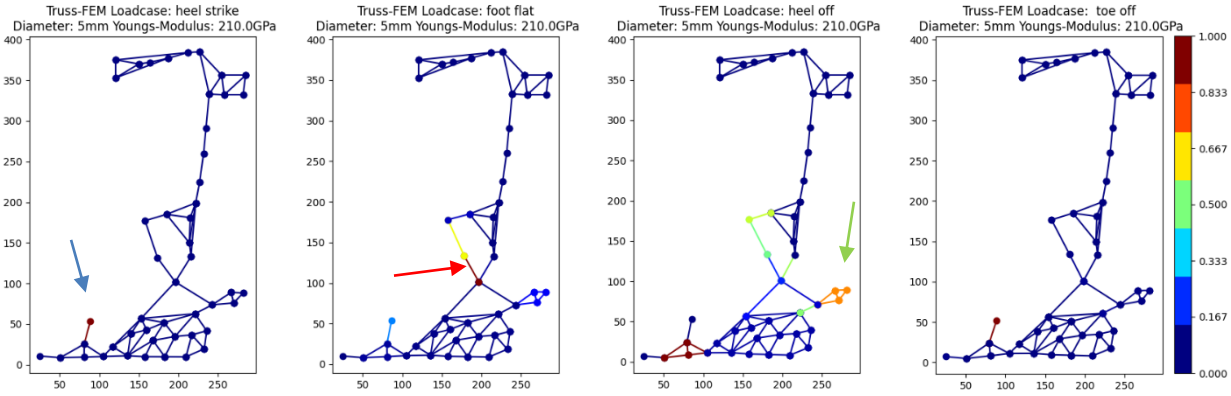

a) b) c) d)

Figure 8. Stress analysis of the 2D truss for the different load cases occurring during walk cycle: a) Heel Strike b) Foot Flat c) Heel Off d) Toe Off

The evaluation of the 2D truss analysis described in Figure 3b) showed that the maximum stresses occurred in the area of the ankle joint for load case foot flat (red arrow). Since the node stiffness works against twisting of the foot section, the largest bending moment is located at the ankle joint and consequently the largest stresses will occur there. Especially in the Foot Flat and Heel Off load cases, the greatest joint reaction forces occur in the gait, which can be seen very clearly in the two middle graphs. At a possible passive energy storage device, which was attached to the right rear area of the orthosis, also high stresses appear (green arrow). The resulting strain could than transfer to body own springs to harvest the appearing energy (see Figure 2 [1]). Within the front area, a type of attachment buckle was designed to stabilize the forefoot during gait and bind it to the orthosis, so the orthosis is always in contact with the foot. This led to high stresses especially during heel strike and toe off (see in Figure 8 a) blue arrow). At the rest of the orthotic area no stress or very little stress compared to the rest occur. Next, the results were used to generate the Figure 5 design space along with the 3D scanning images. This was converted into a B-Rep model and then optimized using the program described in Figure 6. Afterwards, the analysis and optimization of the structure was performed (see Table 1).

Table 1. Comparison of the different process stats of the used element methods.

Parameter	Conventional Tetrahedral Structure	Optimized Truss Structure
Elements	66175	1724
Nodes	111507	3231
CAD Design duration	~2 h	~10 min
Transient FEA Solver	1 h 53 min 40 sec	3 min 51 sec
Optimization Solver	5 min 14 sec	4,84 sec

To solve the transient problem the program Ansys was used. For a conventional tetrahedral discretized structure, the solver needed 1 h 53 min 40 sec. For the same design but discretized with beams the solver

https://doi.org/10.1017/pds.2023.33 Published online by Cambridge University Press

needed 3 min 51 sec. After that a structural optimization was performed. In this process, a target volume of 1724 beams were realized from an initial design space of 3000 beams, which is 54,7 % of the initial design volume. The solver converged after 33 iterations (4.84 sec). A comparable optimality criteria-based topology optimization with shell elements and volume objective function (50%) converged in 40 iterations (5 min. 14 sec). The graphs are not shown due to the similarity of the design suggestions.
Then, the design proposal was loaded into SpaceClaim to assign a constant circular cross-section with a diameter of 5 mm to all beams. The material model was defined as linear elastic with a Young's modulus of 210 ·10³ MPa. The orthosis was then analysed in ANSYS for its deformation and stiffness properties. The results are shown in Figure 9.

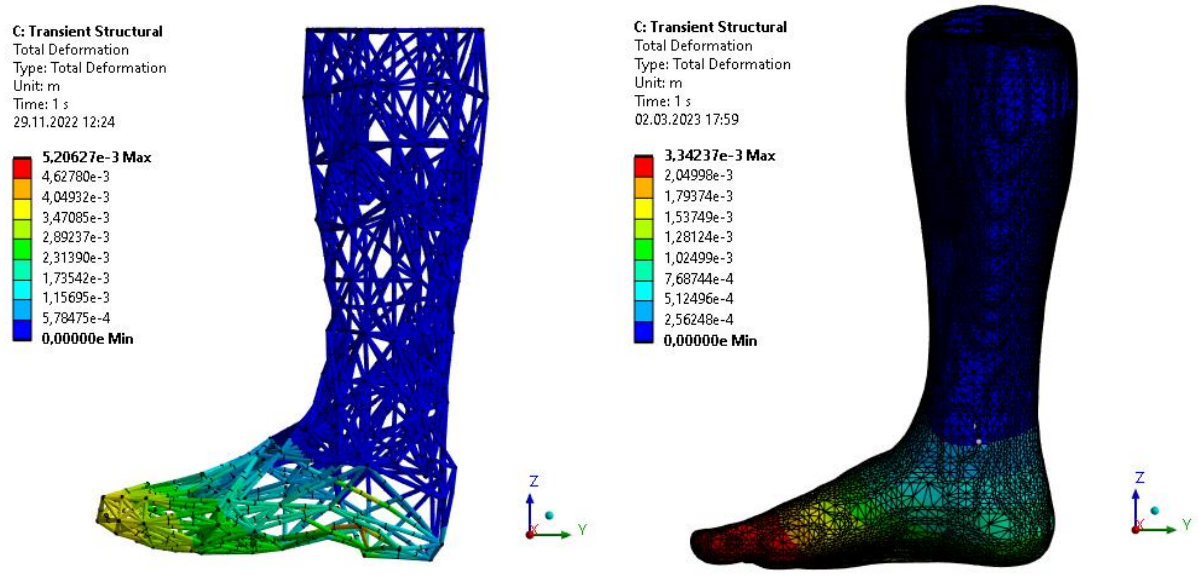

a) b)

Figure 9. Transient structural analysis: Total deformation of the orthosis structure: a) Optimized truss structure b) Tetrahedral discretized structure

The deformation pattern in Figure 9 a) showed a maximum deformation of 5 mm at the toe. As expected, no deformation occurred at the calf fixation. In the heel area, the deformation was also small and occurred, if at all, at beams perpendicular to the direction of force. In contrast to the deformation of the truss structure, the deformation distribution of the tetrahedral model was a bit higher, although the maximum deformation was smaller. However, the overall deformation distribution of both element methods was quite similar.

4 DISCUSSION

The key innovation of this contribution is a fast and efficiently design process for patient specific orthosis. Therefore, established design and analysis methods, tools and programs were substituted with more efficient, simplified and more suitable methods. Here, it comes out, that the rotation of the foot around the upper ankle joint axis causes the temporary spring support at the rear of the foot to shift in a clockwise direction. This insight from the 2D design (see Figure 8) can be used to place energy storage devices such as springs there or to redirect the load to a more suitable location, e.g. colinear to the ankle axis. The deformation plot clearly shows the functionality of truss simulations. Since the same simulation results were obtained for models with higher order elements, it can generally be said that for transient structural calculations of orthoses beam elements can bring a significant saving of resources. Therefore, also a fraction of the time was needed in order to solve the ODE, because of the more simpler element type. However, the assumption that the load is distributed evenly over the entire sole of the foot is only a simplified load case, which has to be defined with more consideration of the variant ankle-moment distribution, over the gait cycle. Regarding the calculation time, however, this is not expected to have any influence. Within the Ansys implicit solver, the time steps and number of substeps are important and not the type and size of the loads. For the pre-processing of the truss structure the CAD-Design-Work were also more less as for the shell structure. As a matter of fact, the build-up of a structure and the various intermediate steps to achieve analysability is dependent on the

https://doi.org/10.1017/pds.2023.33 Published online by Cambridge University Press

prior knowledge, experience and skills of the user/engineer and therefore very subjective. However there are some limitations for the presented design process. The manual discretization of the orthosis structure was not very intuitive and should be improved in the future. Especially in the area of the restraints, automatic meshers can help to generate a continuous mesh. For the cross-sectional area problem, an upstream parameter study can be a solution. The longer calculation times should still be much lower than the design with shell or even solid elements. Furthermore, the beam element bending moment calculations are particularly sensitive to beam diameter/beam area. In a comparative analysis with variable beam diameter for values less than 3.6 mm no convergent solutions exist. Here, the diameter-to-length ratios are so low that the bending stiffnesses become very small and, as a result, the bending moment diverges to infinity.

5 CONCLUSION AND OUTLOOK

The presented method with integrated simplified 3D analysis is a simple, and quick variant for the design of personalized AFOs. Furthermore, the main advantages of the presented method are robustness, due to the already often used design programs and faster convergence of the objective function of the optimization. Since passive orthoses provide great added benefits (Mills *et al.*, 2010), the presented method can be used for educational purposes for future design engineers in the field of personalized medical devices or sports medicine. However, the Method should be than extended by adding mechanical energy storage possibilities like springs. This could be done similar to Tian *et al.* (2015) or by means of alternative actuator technology (Thalman *et al.*, 2022) and the parallel updating of load cases by coupling with MBS-based human model simulations. However, since it is indispensable to perform computations with higher-level elements, a solution must be found for future work to save further computation time. Foremost above a certain structural complexity with possibly executable mechanics and interacting switching processes the computation time will highly increase. When coupling MBS and FEA, the computation times also increase, since in each time step the resulting support reactions in the MBS solver cause new modified load spectra. A possible solution here could be a serially switched model order reduction.

ACKNOWLEDGEMENT

The authors gratefully acknowledge the financial support by the German Research Foundation (DFG) of the projects " Methodology for the design of passive, structure-optimized orthoses for the treatment or compensation of pathophysiological movement patterns using musculoskeletal human models" with the grant numbers WA 2913/43-1 and MI 2608/2-1.

REFERENCES

Ali, M.H., Smagulov, Z. and Otepbergenov, T. (2021), “Finite element analysis of the CFRP-based 3D printed ankle-foot orthosis”, *Procedia Computer Science*, Vol. 179, pp. 55–62.

Andreas Dutzler (2022), “TrussPy Documentation”, available at: https://github.com/adtzlr/trusspy.

Banga, H.K., Kalra, P., Belokar, R.M. and Kumar, R. (2020), “Customized design and additive manufacturing of kids’ ankle foot orthosis”, *Rapid Prototyping Journal*, Vol. 26 No. 10, pp. 1677–1685.

Chu, T.M., Reddy, N.P. and Padovan, J. (1995), “Three-dimensional finite element stress analysis of the polypropylene, ankle-foot orthosis: static analysis”, *Medical Engineering & Physics*, Vol. 17 No. 5, pp. 372–379.

Dhokia, V., Bilzon, J., Seminati, E., Talamas, D.C., Young, M. and Mitchell, W. (2017), “The Design and Manufacture of a Prototype Personalized Liner for Lower Limb Amputees”, *Procedia CIRP*, Vol. 60, pp. 476–481.

Dickinson, A.S., Steer, J.W. and Worsley, P.R. (2017), “Finite element analysis of the amputated lower limb: A systematic review and recommendations”, *Medical Engineering & Physics*, Vol. 43, pp. 1–18.

Fairclough, H.E., He, L., Pritchard, T.J. and Gilbert, M. (2021), “LayOpt: an educational web-app for truss layout optimization”, *Structural and Multidisciplinary Optimization*, Vol. 64 No. 4, pp. 2805–2823.

Hell, S. (2018), *Beiträge zur Analyse und Bewertung von 3D-Spannungssingularitäten mittels einer angereicherten Skalierte-Rand-Finite-Elemente-Methode*, Darmstadt.

Jäger, M. and Wartzack, S. (2023), “Efficient Computation of Spatial Truss Structures for Design Optimization Approaches Using Tube-Shaped Thin-Walled Composite Beams”, in Rieser, J., Endress, F., Horoschenkoff, A., Höfer, P., Dickhut, T. and Zimmermann, M. (Eds.), *Proceedings of the Munich Symposium on Lightweight Design* 2021, Springer Berlin Heidelberg, Berlin, Heidelberg, pp. 1–12.

https://doi.org/10.1017/pds.2023.33 Published online by Cambridge University Press

Kumar Banga, H., Kalra, P., M. Belokar, R. and Kumar, R. (2021), "Design and Fabrication of Prosthetic and Orthotic Product by 3D Printing", in Arazpour, M. (Ed.), *Prosthetics and Orthotics*, IntechOpen, Erscheinungsort nicht ermittelbar.
Leite, M., Soares, B., Lopes, V., Santos, S. and Silva, M.T. (2019), "Design for personalized medicine in orthotics and prosthetics", *Procedia CIRP*, Vol. 84, pp. 457–461.
Mayer, J., Völkl, H. and Wartzack, S. (2022), "Feature-Based Reconstruction of Non-Beam-Like Topology Optimization Design Proposals in Boundary-Representation", in *DS 119: Proceedings of the 33rd Symposium Design for X (DFX2022), 23 September* 2022, The Design Society, p. 10.
Miehling, J. (2019), "Musculoskeletal modeling of user groups for virtual product and process development", *Computer methods in biomechanics and biomedical engineering*, Vol. 22 No. 15, pp. 1209–1218.
Mills, K., Blanch, P., Chapman, A.R., McPoil, T.G. and Vicenzino, B. (2010), "Foot orthoses and gait: a systematic review and meta-analysis of literature pertaining to potential mechanisms", *British Journal of Sports Medicine*, Vol. 44 No. 14, pp. 1035–1046.
Mitternacht, J. and Lampe, R. (2006), "Ermittlung funktioneller kinetischer Parameter aus der plantaren Druckverteilungsmessung", *Zeitschrift fur Orthopadie und ihre Grenzgebiete*, Vol. 144 No. 4, pp. 410–418.
N. P. Reddy, G. Point, P. C. Lam and R. C. Grotz (1985), "Finite element modeling of the ankle-foot orthoses. Proceedings Inter Conf Biomechanics and Clinical Kinesiology of Hand and Foot".
Öchsner, A. (2021), *Classical beam theories of structural mechanics, Springer eBook Collection*, Springer, Cham.
Pahl, G., Beitz, W., Feldhusen, J., Grote, K.-H., Blessing, L.T.M. and Wallace, K. (Eds.) (2007), *Engineering design: A systematic approach*, 3. ed., Springer, London.
Pallari, J., Dalgarno, K.W., Munguia, J., Muraru, L., Peeraer, L., Telfer, S. and Woodburn, J. (2010), *Design and Additive Fabrication of Foot and Ankle-Foot Orthoses*.
Reportlinker (2022), "Prosthetics And Orthotics Market Size, Share & Trend Analysis Report By Type, Prosthetics And Segment Forecasts, 2022 - 2030", 7 November (accessed 18 November 2022).
Scherb, D., Steck, P., Wartzack, S. and Miehling, J. (2022), "Integration of musculoskeletal and model order reduced FE simulation for passive ankle foot orthosis design", Porto.
Shahar, F.S., Hameed Sultan, M.T., Lee, S.H., Jawaid, M., Md Shah, A.U., Safri, S.N.A. and Sivasankaran, P.N. (2019), "A review on the orthotics and prosthetics and the potential of kenaf composites as alternative materials for ankle-foot orthosis", *Journal of the mechanical behavior of biomedical materials*, Vol. 99, pp. 169–185.
Shorter, K.A., Li, Y., Bretl, T. and Hsiao-Wecksler, E.T. (2012), "Modeling, control, and analysis of a robotic assist device", *Mechatronics*, Vol. 22 No. 8, pp. 1067–1077.
Spaeth, J.P. (2006), "Laser imaging and computer-aided design and computer-aided manufacture in prosthetics and orthotics", *Physical medicine and rehabilitation clinics of North America*, Vol. 17 No. 1, pp. 245–263.
Steck, P., Scherb, D., Miehling, J., Völkl, H. and Wartzack, S. (2022), "Synthesis of passive lightweight orthoses considering humanmachine interaction", in *DS 119: Proceedings of the 33rd Symposium Design for X (DFX2022), 23 September* 2022, The Design Society, p. 10.
Štefanovič, B., Michalíková, M., Bednarčíková, L., Trebuňová, M. and Živčák, J. (2021), "Innovative approaches to designing and manufacturing a prosthetic thumb", *Prosthetics and orthotics international*, Vol. 45 No. 1, pp. 81–84.
Syngellakis, S. and Arnold, M.A. (2012), "Modelling considerations in finite element analyses of ankle foot orthoses", in Brebbia, C.A. and Hernandez, S. (Eds.), *Design and Nature VI, 6/11/2012 - 6/13/2012, A Coruna, Spain*, WIT PressSouthampton, UK, pp. 183–194.
Taha, Z., Norman, M.S., Omar, S.F.S. and Suwarganda, E. (2016), "A Finite Element Analysis of a Human Foot Model to Simulate Neutral Standing on Ground", *Procedia Engineering*, Vol. 147, pp. 240–245.
Tavares, J.M.R.S., Bourauel, C., Geris, L. and Vander Slote, J. (2023), *Computer Methods, Imaging and Visualization in Biomechanics and Biomedical Engineering II: Selected Papers from the 17th International Symposium CMBBE and 5th Conference on Imaging and Visualization, September 7-9, 2021, Springer eBook Collection*, Vol. 38, 1st ed. 2023, Springer International Publishing; Imprint Springer, Cham.
Thalman, C.M., Hertzell, T., Debeurre, M. and Lee, H. (2022), "Multi-degrees-of-freedom soft robotic ankle-foot orthosis for gait assistance and variable ankle support", *Wearable Technologies*, Vol. 3, e18.
Tian, F., Hefzy, M.S. and Elahinia, M. (2015), "State of the art review of knee-ankle-foot orthoses", *Annals of biomedical engineering*, Vol. 43 No. 2, pp. 427–441.
Totah, D., Kovalenko, I., Saez, M. and Barton, K. (2017), "Manufacturing Choices for Ankle-Foot Orthoses: A Multi-objective Optimization", *Procedia CIRP*, Vol. 65, pp. 145–150.
Wang, Y., Li, Z., Wong, D.W.-C., Cheng, C.-K. and Zhang, M. (2018), "Finite element analysis of biomechanical effects of total ankle arthroplasty on the foot", *Journal of Orthopaedic Translation*, Vol. 12, pp. 55–65.
Wong, D.W.-C., Niu, W., Wang, Y. and Zhang, M. (2016), "Finite Element Analysis of Foot and Ankle Impact Injury: Risk Evaluation of Calcaneus and Talus Fracture", *PloS one*, Vol. 11 No. 4, e0154435.

https://doi.org/10.1017/pds.2023.33 Published online by Cambridge University Press